Efficient Analysis of Switchable FSS Structure using the WCIP Method

N. Sboui[1], A. Salouha[1], L. Latrach[1], A. Gharsallah[1], A. Gharbi[1], and H. Baudrand[2]

[1]Laboratoire d'Electronique Département de Physique
Faculté des Sciences de Tunis, 2092 El Manar Tunisia
noureddine.sboui@fst.rnu.tn

[2]Laboratoire d'Electronique
EN SEEIHT de Toulouse France

***Abstract*—**A precise technique based on the wave concept iterative procedure (WCIP) and a fast mode transformation (FMT) is used to adjust the frequency selective surface (FSS) response. This adjustment is achieved by integrating RF-MEMS switches. These systems use the manufacturing processes of integrated circuits. In order to initialize the iterative procedure, an incident wave is defined in spectral domain. The numerical results are compared to those obtained with the finite element method (FEM). The good agreement between simulated and published data justifies the design procedure.

Index Terms — FSS, MEMS RF, 2D-FFT algorithm.

I. INTRODUCTION

The frequency selective surfaces (FSS) are printed by surfaces composed of a periodic metallic circuit or openings in a circuit plane. They can be periodic along one or two directions [1-3]. They provide a reflection or total transmission of signals in certain frequency bands [4-5]. We can adjust this frequency of resonance by integrating a PIN diode, FET, or RF MEMS switch. The semiconductor switches are used first. They present some limitation in terms of energy consumption, insertion loss and cut-off frequency. The RF-MEMS switches are devices that use a mechanical movement to assign a switching of the RF transmission line [6-8]. The principal advantages of the RF-MEMS switches are low consumption, low insertion loss and quality factor [3]. Their application areas are extensive and always tend to grow. The most used switching techniques are the air bridge technology and technique of micro beam [9-10].

The contact switch is the equivalent of the RF-MEMS switch. It has two states of commutation: the state ''off'' and the state ''on''. In a blocked state, the switch has a capacitive behavior, with the state passing; it is comparable to a resistance representing the losses of a metal/metal contact.

We can distinguish several categories of components from this technology; our study will focus on the resistive switch (cantilever). Indeed these components have many advantages compared to their direct competitors, semi-conductors: reduced losses, more compact and passive components.

Simulation is an essential step in modeling this type of circuit. In this framework, several analytical methods have been developed. Among these methods that already exist, we present in what follows a new iterative method based on the wave concept. This method has major advantages over other methods. These advantages are concerning, in special, the execution velocity of the resolution procedure and the arbitrary form of the under studied structure. Besides this iterative technique uses a rapid transformation FMT which ensures a rapid transition between the spectral and spatial domain [11-12]. We combine the wave concept with the two dimensions fast Fourier transformation (2D-FFT) algorithm to change the domain. The use of the 2D-FFT algorithm is required to mesh the circuit plane into 2D small rectangular pixels. Hence, the boundary conditions are satisfied at each pixel. By using the 2D-FFT algorithm, a high computational speed can be achieved [13].

The purpose of this paper is to extend the wave concept iterative process (WCIP) method to the analysis of the integration of microsystems

Submitted On: Oct. 8, 2010
Accepted On: Feb. 11, 2011

performance (MEMS) in circuit materials periodic FSS (infinite number of unit cells) with arbitrary angle of incidence in the one layer configuration of dielectrics [3]. Two different examples are studied, switchable split-ring FSS and switched-beam antenna. For both cases, our simulation results are validated with published data.

II. THEORY

Let us consider a periodic arbitrary one-layer structure, Fig. 1 shows the unit cell of periodic circuit.

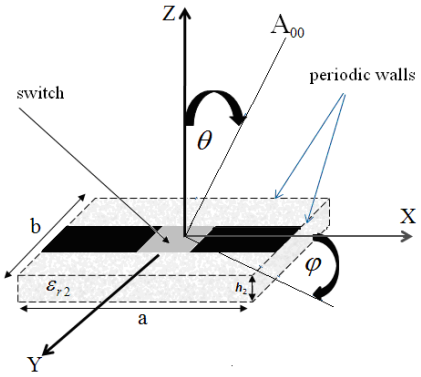

Fig. 1. Unit cell of the periodic structure with arbitrary incidence A_{00}.

This interface can support the circuit and includes three sub-domains metal M_i, dielectric D_i, and switch SW_i. We consider that the electromagnetic field is known on all points of the plane interface [7]. The solution of the problem has to satisfy the following boundary conditions:

$$\begin{cases} E_{T1} = E_{T2} = 0 & Metal(M) \\ J_T = J_{T1} + J_{T2} & Dielectric(D) \\ J_{sw} = y_{sw} E_{sw} & Switch(SW) \end{cases} \quad (1)$$

In equation (1), E_{T1} and E_{T2} are the tangential components of the electric field at media (1) and (2), respectively, and JT1 and JT2 are the corresponding current density. E_{SW}, J_{SW}, and y_{SW} are the electric field, the current density, and the admittance equivalent circuit of the switch domain respectively.

In the last domain, the electric field and the current density are related to the potential and electric current as follows:

$$E_{sw} = \frac{V_1}{G} \quad ; \quad J_{sw} = \frac{I}{W} . \quad (2)$$

This enables us to write

$$\frac{J_{sw}}{E_{sw}} = \frac{I}{V_1}\left(\frac{G}{W}\right) = Y_{sw}\left(\frac{G}{W}\right) = y_{sw} . \quad (3)$$

As shown on Fig. 2, the incident waves A_i and the scattering waves B_i are given in the terms of the transverse electric E_{Ti} and magnetic fields H_{Ti} at the circuit interface (Ω). This leads to the following set of equations:

$$\begin{cases} A_i = \dfrac{\sqrt{y_{0i}}}{2}\left(E_{Ti} + \dfrac{1}{y_{0i}}(H_{Ti} \times n)\right) \\ B_i = \dfrac{\sqrt{y_{0i}}}{2}\left(E_{Ti} - \dfrac{1}{y_{0i}}(H_{Ti} \times n)\right) \end{cases} \quad (4)$$

where y_{0i} is an intrinsic admittance characterizing the medium, i denotes the two media beside Ω (i=1 and 2), which can be defined as: $y_{0i} = \sqrt{\dfrac{\varepsilon_0 \varepsilon_{ri}}{\mu}}$ with ε_0, μ_0, and ε_{ri} are the permittivity and permeability of the vacuum and the relative permittivity of the medium 'i' respectively. n is the outward vector normal to the interface.

The surface current density is introduced as being $J_{Ti} = H_{Ti} \times n$.

On the dielectric:

$$\left\{\begin{vmatrix} B_1 \\ B_2 \end{vmatrix} = \left[S_D \right] \begin{vmatrix} A_1 \\ A_2 \end{vmatrix}\right\}_{x,y} , \quad (5)$$

$$\left[S_D\right] = \begin{bmatrix} \dfrac{1-n_{12}}{1+n_{12}} & \dfrac{2n_{12}}{1+n_{12}} \\ \dfrac{2n_{12}}{1+n_{12}} & -\dfrac{1-n_{12}}{1+n_{12}} \end{bmatrix}, \quad (6)$$

where $n_{12} = \dfrac{y_{01}}{y_{02}}$.

On the switch:

$$\left\{\begin{vmatrix} B_1 \\ B_2 \end{vmatrix} = \left[S_{SW} \right] \begin{vmatrix} A_1 \\ A_2 \end{vmatrix}\right\}_{x,y} , \quad (7)$$

$$\left[S_{SW}\right] = \begin{bmatrix} \dfrac{-1-n_{s1}+n_{s2}}{1+n_{s1}+n_{s2}} & \dfrac{2n_s}{1+n_{s1}+n_{s2}} \\ \dfrac{2n_s}{1+n_{s1}+n_{s2}} & -\dfrac{1+n_{s1}-n_{s2}}{1+n_{s1}+n_{s2}} \end{bmatrix},$$

$$n_{s1} = \frac{y_{sw}}{y_{01}}, \; n_{s2} = \frac{y_{sw}}{y_{02}} \; and \; n_s = \frac{\sqrt{y_{01} y_{02}}}{y_{sw}} .$$

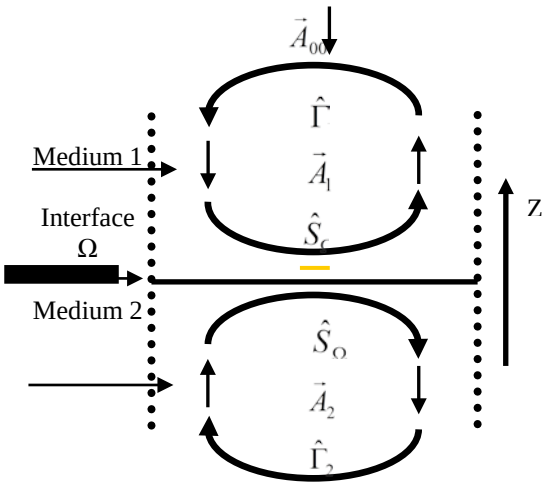

Fig. 2. Definition of waves for the single-layer structure.

With equations (5), (6), and (7), we deduce the global spatial equation that relates the incident waves on all the interfaces.

$$\left\{\begin{vmatrix} B_1 \\ B_1^{'} \end{vmatrix} = [S] \begin{vmatrix} A_1 \\ A_1^{'} \end{vmatrix}\right\}_{x,y}, \tag{8}$$

where:

$$[S] = \hat{H}_M [S_M] + \hat{H}_D [S_D] + \hat{H}_{SW} [S_{SW}] + A_{00},$$

and

$$\hat{H}_\pi = \begin{cases} 1 & if \quad \pi = M_i, D_i \text{ or } SW_i \\ 0 & else\ where \end{cases}.$$

Between medium 1 and 2, the waves are defined in the spectral domain (TE and TM modes). Then, the spectral equations describe the waves behaviour is defined as [4].

$$\left\{A_i = \hat{\Gamma}_i B_i\right\}_\alpha, \tag{9}$$

$$\hat{\Gamma}_{i\alpha} = \frac{Z_{mni\,\alpha} - z_{0i}}{Z_{mni\,\alpha} + z_{0i}}, \tag{10}$$

where, i=1,or 2 and $Z_{mni\,\alpha}$ is the impedance of the mn-th mode at the medium i and α stands for the modes TE or TM.

where: $Z_{mni\,TE} = \frac{j\omega\mu_0}{\gamma_{mni}}$, $Z_{mni\,TM} = \frac{\gamma_{mni}}{j\omega\varepsilon_0\varepsilon_{ri}}$

γ_{mni} being the propagation constant of the medium i and it is given by

$$\gamma_{mni} = \sqrt{\beta_{xm}^2 + \beta_{yn}^2 - k_0^2 \varepsilon_{ri}},$$

$$k_0 = \omega\sqrt{\mu_0\varepsilon_0}, \omega = 2\pi\frac{c}{\lambda},$$

$$\beta_{xm} = \beta_x + \frac{2m\pi}{a}, \beta_{yn} = \beta_y + \frac{2n\pi}{b}.$$

$$\beta_x = \omega\sqrt{\varepsilon_{r1}\mu_{r1}}\sqrt{\varepsilon_0\mu_0}\sin\theta\cos\varphi,$$

$$\beta_y = \omega\sqrt{\varepsilon_{r1}\mu_{r1}}\sqrt{\varepsilon_0\mu_0}\sin\phi\cos\theta.$$

(a) and (b) are the periodicity along (ox) and (oy), respectively, θ and φ define the angle of incidence.

We deduce that the global spectral equation relates the diffracted wave A_i to incident B_i one in the spectral domain.

$$A_i^{k+1} = \hat{\Gamma}_i B_i^{(k)} + A_0. \tag{11}$$

In the above equation, we have included the excitation wave $A_{00} = \begin{vmatrix} A_{ox} \\ A_{oy} \end{vmatrix}$. A_{00} is defined in the spectral domain and has the following expression:

For TE polarization:

$$\begin{cases} A_{0x} = \frac{1}{2\sqrt{Z_{oi}}} \frac{\beta_y}{\sqrt{|\beta_x|^2 + |\beta_y|^2}} \frac{1}{\sqrt{ab}} e^{-j(\beta_x x + \beta_y y)} \\ A_{0y} = \frac{-1}{2\sqrt{Z_{oi}}} \frac{\beta_x}{\sqrt{|\beta_x|^2 + |\beta_y|^2}} \frac{1}{\sqrt{ab}} e^{-j(\beta_x x + \beta_y y)} \end{cases}. \tag{12}$$

For TM polarization:

$$\begin{cases} A_{0x} = \frac{-1}{2\sqrt{Z_{oi}}} \frac{\beta_x}{\sqrt{|\beta_x|^2 + |\beta_y|^2}} \frac{1}{\sqrt{ab}} e^{-j(\beta_x x + \beta_y y)} \\ A_{0y} = \frac{1}{2\sqrt{Z_{oi}}} \frac{\beta_y}{\sqrt{|\beta_x|^2 + |\beta_y|^2}} \frac{1}{\sqrt{ab}} e^{-j(\beta_x x + \beta_y y)} \end{cases}. \tag{13}$$

III. APPLICATIONS

The RF MEMS switches are mechanically deformable micro switches. In the first step of this first example, we studied FSS a screen which integrates a PIN diode into two borderline cases (short-circuit and open circuit), as shown in Fig. 3.

The structure is excited by a plane wave with normal incidence. The physical parameters are the following: height of the substrate h=0.6mm its permittivity ε_r=3. The unit cell dimension are a=b=40mm. The microstrip line length L=40mm and its width W=1mm, as shown in Fig. 3.

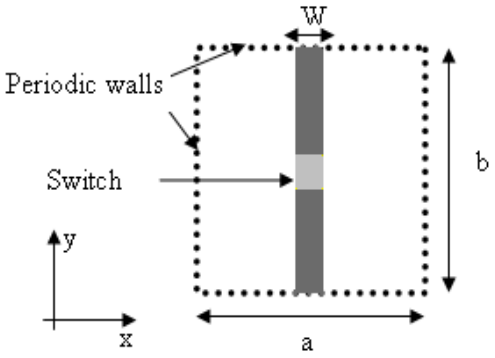

Fig. 3. Resistive switch inserted on a microstrip line.

The convergence according to the iteration count presented in Fig. 4 is obtained from 50 iterations.

For the short circuit case, the simulation results of the transmission coefficient, as a function of frequency, is shown in Fig. 5. This shows that there is a total transmission signal. This result compared to [15], shows there is a good agreement with the iterative method.

In the open circuit case, one can conclude from the simulation result presented in Fig. 6 that the gap has given rise to a band gap in a well determined frequency. In fact in our simulation, we use only a gap where a pin diode in the gap state is used [15]. This explains the difference in bandwidth between the two results.

As a consequence of this important aspect, elements are inserted into the gap to achieve switching DC-electric and have thereby controlling electronic structures, FSS, changing their behavior between the response of discontinuous and continuous elements.

For different values of the capacitor, we present, in Figs. 7 to 9, the results of simulations of transmission coefficients as a function of frequency. In these figures, we clearly distinguish the effect of integration of the switch to the off state. We notice the changes in the resonant frequency when the capacitance changes.

The results presented by the iterative method are in agreement with those published by the finite element method (FEM).

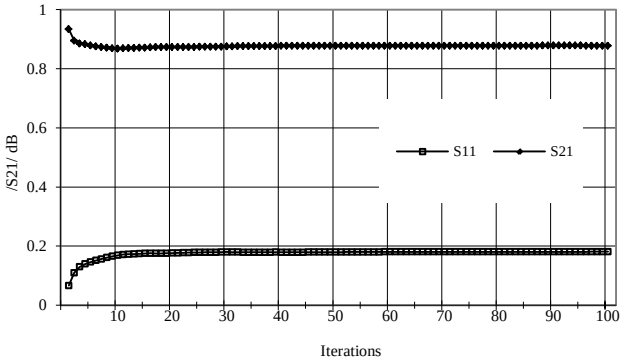

Fig. 4. Convergence of the S parameters as function of iterations number at 7 GHz.

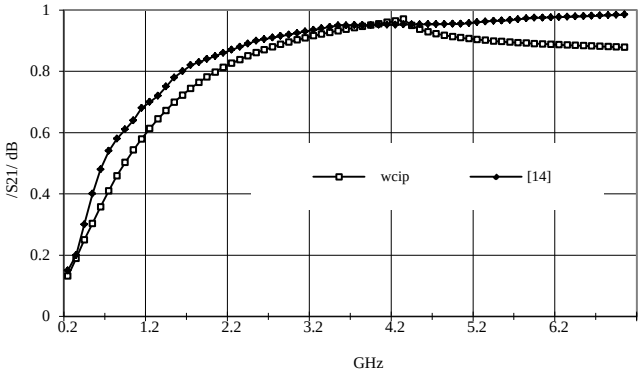

Fig. 5. Variation of transmission coefficient as function of frequency (short circuit case).

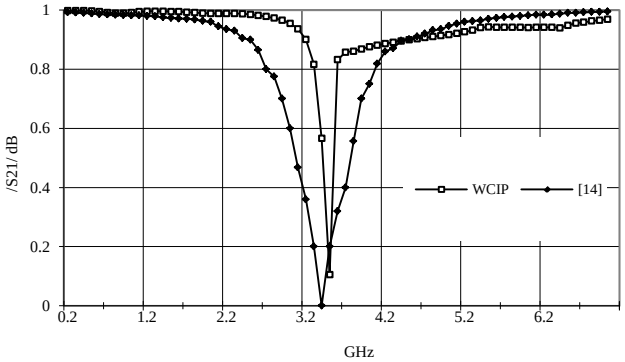

Fig. 6. Variation of transmission coefficient as function of frequency (open circuit case).

In the second example, we integrate three capacitive switches between two rings of split-ring resonator (SRR), as shown in Fig. 10. At first, we consider the ON state of all of the three switches.

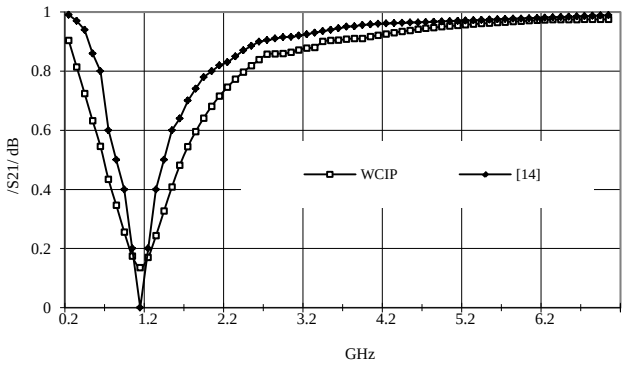

Fig. 7. Variation of transmission coefficient as a function of frequency c=1pF.

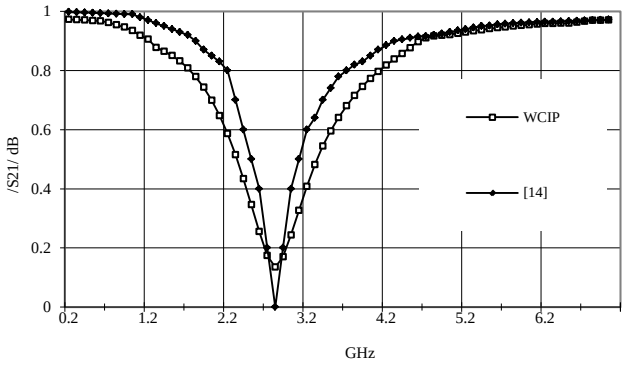

Fig. 8. Variation of transmission coefficient as a function of frequency c=100pF.

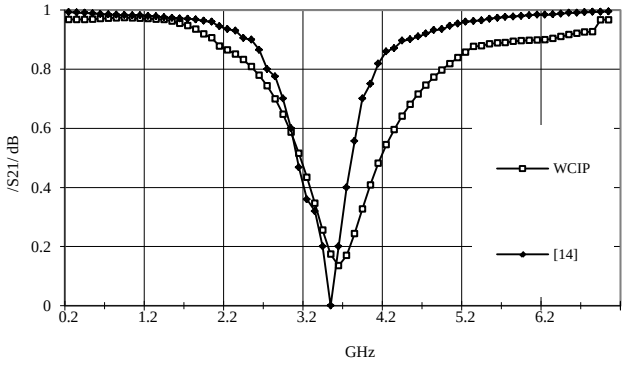

Fig. 9. Variation of transmission coefficient S_{21} as a function of frequency c=0pF.

As shown in Fig. 11, we find that the transmission coefficient obtained using the iterative method is about -22 dB at 4.64GHz. These results refer to those obtained by the FEM [15].

The second phase consists of integrating two capacitors' switches and a resistive switch into the place of the metal packing, to be able to distinguish the effect of integration from the switches between the rings of the resonator. Two cases will be presented, the first case or the three switches has state off, and the three switches (S1, S2, and S3) take the values, respectively, (0.3pf, 0.3pf, and 1 Ω).

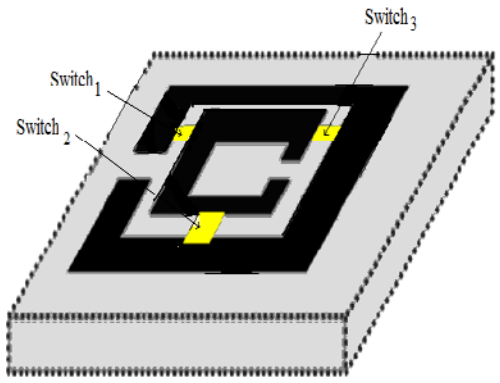

Fig. 10. Two enclosed rings with three switches (S1, S2, S3).

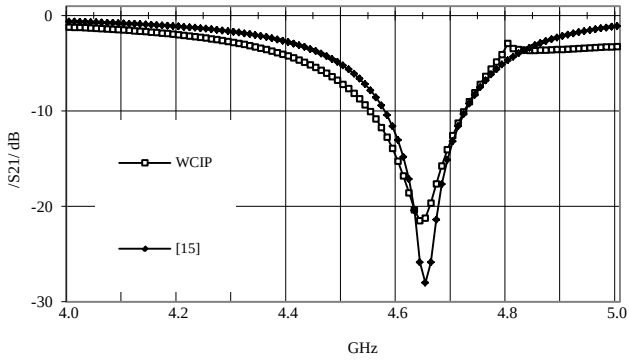

Fig. 11. Variation of transmission coefficient as a function of frequency.

Figure 12 presents the coefficient of transmission in dB and suggests the frequency of resonance to 4.57 GHz with a transmission of about -28 dB. The state ''ON'' the three switches (S1, S2, and S3) takes successively the values (1pf, 1pf, and 5 Ω).

Figure 13 presents the coefficient of transmission in dB and shows a frequency of resonance to 4.57 GHz with a transmission of about -23 dB.

Figure 14 enables us to distinguish the difference between the various cases from commutations (S1, S2,

and S3) compared to the answer of metal modeling obtained by the iterative method.

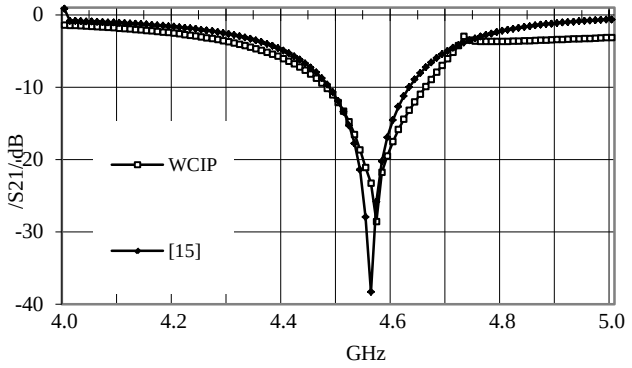

Fig. 12. Variation of transmission coefficient as a function of frequency with C1=C2=0.3pF and R=1Ω.

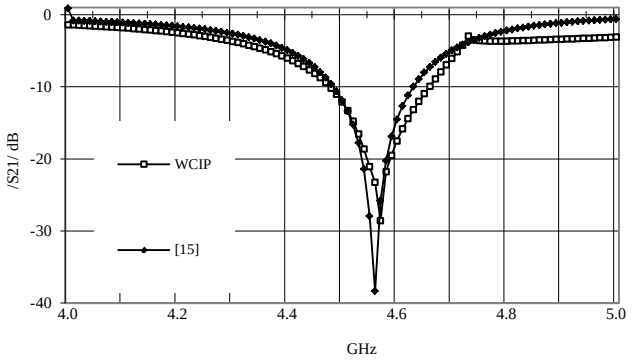

Fig. 13. Variation of transmission coefficient as a function of frequency with C1=C2=1pF and R=5Ω.

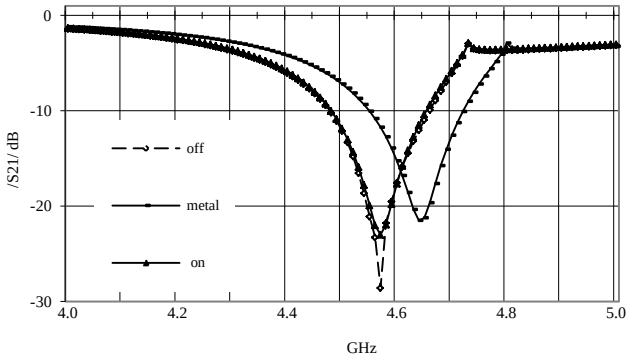

Fig. 14. Variation of transmission coefficient as a function of frequency.

IV. CONCLUSION

In this paper, a reformulation of the wave concept iterative method is reformulated to the integrated RF-MEMS switch. The convergence of the procedure is about 100 iterations. The comparison of numerical results with the measurement published data verified the validation of the WCIP method to integrating the RF Switch. This method has the advantage of simplicity and its conjunction with the 2D-FFT allows a high computational speed and memory consumption.

REFERENCES

[1] B. A. Munk, *Frequency Selective Surfaces: Theory and Design*, John Wiley & Sons, New York, 2000.

[2] R. Mittra, C. H. Chan, and T. Cwik, "Techniques for Analysing Frequency Selective Surfaces - A Review," *Proc. IEEE*, vol. 76, pp. 1593-1615, 1988.

[3] G. M. Rebeiz, *RF MEMS: Theory, Design, and Thechnologie,* Wiley-Interscience, 1st Edition, June 2002.

[4] L. Latrach, N. Sboui, A. Gharsallah, A. Gharbi, and H. Baudrand, "Analysis and Design of a Planar Multilayered FSS with Arbitrary Incidence," *Applied Computational Electromagnetics Society (ACES) Journal*, vol. 23, no. 2, pp. 149-154, 2008.

[5] H. Oraizi and M. Afsahi, "Analysis of Planar Dielectric Multilayers as FSS by Transmission Line Transfer Matrix Method (TLTMM)," *Progress In Electromagnetics Research*, vol. 74, pp. 217-240, 2007.

[6] M. Hosseini, A. Pirhadi, and M. Hakkak, "A Novel AMC with Little Sensitivity to the Angle of Incidence Using 2-Layer Jerusalem Cross FSS," *Progress In Electromagnetics Research*, PIER 64, pp. 43-51, 2006.

[7] N. Sboui, A. Gharsallah, H. Baudrand, and A. Gharbi, "Design and Modeling of RF MEMS Switch by Reducing the Number of Interfaces," *Microwave and Optical Technology Letters*, vol. 4913, no. 5, pp. 1166-1170, May 2007.

[8] H-P. Tsai, Y. Wang, and T. Itoh, "An Unconditionally Stable Extended (USE) Finite-Element Time-Domain Solution of Active Nonlinear Microwave Circuits using Perfectly Matched Layers," *IEEE Trans. Microwave Theory and Techniques*, vol. 50, pp. 2226-2232, Oct. 2002.

[9] A. Abbaspour-Tarnijani, L. Dussopt, and G.M. Rebeiz, "A High Performance MEMS Miniature Tuneable Bandpass Filter," *IEEE MTT-S International Microwave Symposium Digest*, vol. 3, pp. 1785-1788, 2003.

[10] M. A. Habib, M. N. Jazi, A. Djaiz, M. Nedil, and T. A. Denidni, "Switched-Beam Antenna Based on EBG Periodic Structures," *Microwave Symposium Digest, IEEE MTT-S International*, 2009.

[11] N. Sboui. A. Gharsallah, H. Baudrand, and A. Gharbi, "Analysis of Double Loop Meander Line by using Iterative Process," *Micro. and Opt. Techn. Lett.*, vol. 26, no. 6, pp. 396-399, Sep. 2000.

[12] H. Baudrand, N. Raveu, N. Sboui, and G. Fontgalland, "Applications of Multiscale Waves Concept Iterative

Procedure," *Inter. Microw. and Opt. Conference*, Salvador, Brazil, October 29-November 1, 2007.

[13] L. Latrach, N. Sboui, A. Gharsallah, A. Gharbi, and Henri Baudrand, "Design and Modelling of Microwave Active Screen Using a Combination of the Rectangular and Periodic Waveguides Modes," *Journal of Electromagnetic Waves and Applications*, vol. 23, no. 11-12, pp. 1639-1648, 2009.

[14] M. A. Habib, M. N. Jazi, A. Djaiz, M. Nedil, and T. A. Denidni, "Switched-Beam Antenna Based on EBG Periodic Structures," *Microwave Symposium Digest, IEEE MTT-S International*, 2009.

[15] M. H. B. Ucar, A. Sondas, and Y. E. Erdemli, "Switchable Splitring Frequency Selective Surface," *Progress In Electromagnetics Research B*, vol. 6, pp. 65-79, 2008.